OPEN

Original article

Nuclear Medicine Communications

Improving quantitative dosimetry in ^{177}Lu-DOTATATE SPECT by energy window-based scatter corrections

Robin de Nijs[a], Vera Lagerburg[b,c], Thomas L. Klausen[a] and Søren Holm[a]

Purpose **Patient-specific dosimetry of lutetium-177 (^{177}Lu)-DOTATATE treatment in neuroendocrine tumours is important, because uptake differs across patients. Single photon emission computer tomography (SPECT)-based dosimetry requires a conversion factor between the obtained counts and the activity, which depends on the collimator type, the utilized energy windows and the applied scatter correction techniques. In this study, energy window subtraction-based scatter correction methods are compared experimentally and quantitatively.**

Materials and methods **^{177}Lu SPECT images of a phantom with known activity concentration ratio between the uniform background and filled hollow spheres were acquired for three different collimators: low-energy high resolution (LEHR), low-energy general purpose (LEGP) and medium-energy general purpose (MEGP). Counts were collected in several energy windows, and scatter correction was performed by applying different methods such as effective scatter source estimation (ESSE), triple-energy and dual-energy window, double-photopeak window and downscatter correction. The intensity ratio between the spheres and the background was measured and corrected for the partial volume effect and used to compare the performance of the methods.**

Results **Low-energy collimators combined with 208 keV energy windows give rise to artefacts. For the 113 keV energy window, large differences were observed in the ratios for the spheres. For MEGP collimators with the ESSE correction technique, the measured ratio was close to the real ratio, and the differences between spheres were small.**

Conclusion **For quantitative ^{177}Lu imaging MEGP collimators are advised. Both energy peaks can be utilized when the ESSE correction technique is applied. The difference between the calculated and the real ratio is less than 10% for both energy windows. *Nucl Med Commun* 35:522–533 © 2014 Wolters Kluwer Health | Lippincott Williams & Wilkins.**

Nuclear Medicine Communications 2014, **35**:522–533

Keywords: ^{177}Lu, comparison, dosimetry, DOTATATE, energy windows, scatter correction, SPECT

[a]Department of Clinical Physiology, Nuclear Medicine and PET, Rigshospitalet, Copenhagen University Hospital, Copenhagen, Denmark, [b]Department of Clinical Physics, Spaarne Hospital, Hoofddorp and [c]Department of Medical Physics, Catharina Hospital, Eindhoven, The Netherlands

Correspondence to Robin de Nijs, MSc, PhD, Department of Clinical Physiology, Nuclear Medicine and PET, Rigshospitalet, Copenhagen University Hospital, Section 4.01.2, Blegdamsvej 9, DK-2100 Copenhagen, Denmark
Tel: +45 3545 4011; fax: +45 3545 4015; e-mail: robin.de.nijs@regionh.dk

Received 11 November 2013 **Revised** 18 December 2013
Accepted 18 December 2013

Introduction

One of the treatment options for neuroendocrine tumours is peptide receptor radionuclide therapy with lutetium-177 (^{177}Lu)-DOTATATE, which contains the octreotide derivative (Tyr^3)-octreotate in its molecular structure. It will bind to the somatostatin receptors, which overexpress in these types of tumours [1]. The combination of β-radiation and γ-radiation makes ^{177}Lu an interesting choice for this treatment. β-Radiation is necessary for therapy, whereas γ-radiation makes imaging of the therapy (uptake) possible. Ideally, a dose as high as possible is given to the tumour, whereas the surrounding organs receive a dose as low as possible. In ^{177}Lu-octreotide treatments, the uptake of the tracer differs across patients, which influences the dose to the neighbouring organs as well. Therefore, in order to obtain optimal treatment, patient-specific dosimetry is necessary. Knowledge about dose response in peptide receptor radionuclide therapy is still limited, mainly because there continue to be considerable uncertainties in dose calculation [2]. The method used to perform lutetium-octreotide dosimetry varies considerably [3–5], which makes it difficult to compare treatment outcome and complication rates depending on the administered dose. In order to perform accurate dosimetry a conversion factor is necessary between the obtained counts in a single photon emission computer tomography (SPECT) image and the real activity.

^{177}Lu has two main photon energy peaks that could be used for imaging and therefore for dosimetry: one at 208 keV and one at 113 keV. Low-energy collimators are normally suitable only for energies below 160 keV. When isotopes with a higher photon energy are used, septal penetration will occur, which can give rise to star artefacts. This makes low-energy collimators unsuitable for imaging the 208 keV photons of ^{177}Lu. Because the 208 keV peak has a higher incidence (10.4%) compared with that of 113 keV (6.8%) and in addition a slightly

0143-3636 © 2014 Wolters Kluwer Health | Lippincott Williams & Wilkins

DOI: 10.1097/MNM.0000000000000079

Fig. 1

The 10-l acylic phantom (dimensions 24.1 × 30.5 × 24.1 cm) with six spheres of inner diameters 10, 13, 17, 22, 28 and 37 mm. The phantom is described in NEMA NU2-2007, section 7 'Image quality accuracy of attenuation and scatter corrections'. Image courtesy of PTW (Physikalisch-Technische Werkstätten).

lower attenuation in the tissue, it is more suitable for imaging, and therefore normally medium-energy general purpose (MEGP) collimators are used for imaging with ^{177}Lu. Many centres use only the higher energy peak because of downscatter from the 208 keV peak into the 113 keV window. This can originate from scatter in the patient and backscatter into the crystal, as 180° scattering of 208 keV photons gives rise to 115 keV photons. Further, at Rigshospitalet, at present only the high-energy peak is utilized for imaging, combined with an MEGP collimator and the standard scatter correction [effective scatter source estimation (ESSE)].

Acquiring data from the 113 keV window in addition to the 208 keV window will improve the count statistics and thus might also increase contrast resolution, which makes more accurate dosimetry or shorter scanning time possible. Appropriate scatter correction techniques have to be applied in order to be able to use both windows.

Several methods exist for scatter correction – for example, energy window subtraction methods [6–11], convolution subtraction methods [12] and limitation of the detection of scattered photons by, for example, changing the energy window [7]. In this study different (down)scatter correction techniques, relying on energy window subtraction, were compared with each other for three different collimators in an experimental ^{177}Lu SPECT study to find the optimal situation for dosimetry in ^{177}Lu imaging. In a study by Beauregard *et al.* [13] one energy window subtraction method with medium-energy collimators was investigated for the 208 keV window. It is hypothesized that quantitatively accurate ^{177}Lu SPECT can be achieved using both energy windows when the appropriate combination of collimator and scatter correction technique is used.

Materials and methods

A 10-l acrylic phantom (NEMA2007/IEC2008) with six fillable spheres (inner diameter: 37, 28, 22, 17, 13 and 10 mm; wall thickness: ∼1 mm) was filled with a ^{177}Lu solution (Fig. 1). The hollow spheres were filled with a higher activity concentration than the uniform background activity concentration, resulting in hot spots. Two samples were removed from the background and from the largest of the spheres to perform accurate counting in a calibrated gamma counter (Packard Cobra II Auto Gamma; Perkin-Elmer, Waltham, Massachusetts, USA). The true intensity ratio between the spheres and the background was calculated on the basis of these measurements. The absolute activity concentration in the spheres at the beginning of the first scan was 1.31 MBq/ml, and the sphere-to-background concentration ratio was 12.88. These activity concentrations are comparable to the activity concentration in normal clinical practice; a homogeneous distribution of 7.4 GBq ^{177}Lu in a 70 kg patient gives a concentration of ∼0.1 MBq/ml, which was used as the background concentration in the phantom. Tumours can have an activity concentration of the order 1 MBq/ml or higher, and kidneys typically have an uptake on the order of 0.5 MBq/ml 1 day after administration.

Experiments were performed using a dual-head 16-slice computer tomography (CT) Philips Precedence SPECT/16MDCT scanner (Philips Healthcare, Best, the Netherlands) with a 9.5-mm-thick scintillation crystal. SPECT scans were consecutively acquired within 3 h with three different collimators (in this order): low-energy high resolution (LEHR), MEGP and low-energy general purpose (LEGP). Table 1 shows the specifications of the collimators. Scans were acquired over 360° at 128 angles (30 s/angle, step and shoot mode) in a 128 × 128 matrix size with a pixel size of 3.195 mm and an orbit radius of 25 cm. The time interval between the starting times of the three scans was ∼1 h. Fifteen different energy windows were defined (Fig. 2 and Table 2). Two main energy windows were defined, one at 113 keV and one at 208 keV, both with a 20% width. In order to obtain the appropriate energy windows some of the acquired energy windows in Table 2 need to be added and/or subtracted before applying the energy window-based correction methods described in the next section; for example, the upper half of the photo peak at 208 keV can be obtained by subtracting window 15 from window 1. Reconstruction for all scans and all collimators was performed with the Philips Astonish reconstruction technique. This is a technique based on ordered subset expectation maximization with a depth-dependent resolution recovery method [14]. Reconstruction was performed with three iterations and eight subsets as recommended by the vendor. In order to investigate the possible influence of the number of iterations and subsets, some of the reconstructions for the LEHR collimator were also

Table 1 Collimator specifications according to product sheet

Collimator names	Hole size	Hole length	Septa thickness	Relative sensitivity[a]	System resolution FWHM at 10 cm[b]	Septal penetration (%)[c]
LEHR	1.40	32.8	0.152	0.55	7.4	1.3
LEGP	1.40	24.7	0.180	1.0[d]	8.8	1.9
MEGP	2.95	48.0	1.143	0.8[e]	11.3	3.3

All collimators have hexagonal hole shape. All sizes in mm.
FWHM, full width at half maximum; LEHR, low-energy high resolution; LEGP, low-energy general purpose; MEGP, medium-energy general purpose.
[a]Compared with LEGP for ^{99m}Tc, 20% energy windows.
[b]For a 9.5-mm-thick crystal.
[c]Septal penetration of respectively 140 keV photons for the low-energy collimators and of 300 keV photons for the medium-energy collimators.
[d]265 cpm/μCi = 119 cps/MBq.
[e]Measured ratio for ^{99m}Tc.

Fig. 2

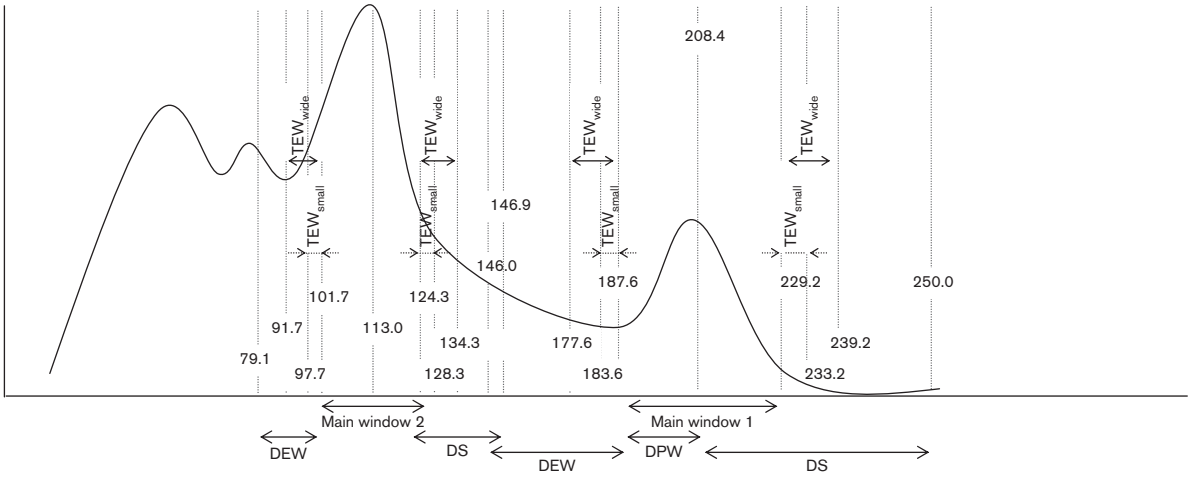

The acquired energy windows, see Table 2. DEW, dual-energy window; DS, downscatter; DPW, dual-photopeak window; TEW, triple-energy window.

Table 2 The acquired energy windows and their description

Window numbers	Lower energy limit (keV)	Upper energy limit (keV)	Description	Abbreviation
1	187.6	229.2	Main window 1	
2	101.7	124.3	Main window 2	
3	177.6	187.6	TEW 1	TEW_{wide}
4	229.2	239.2	TEW 1	TEW_{wide}
5	183.6	187.6	TEW 1	TEW_{small}
6	229.2	233.2	TEW 1	TEW_{small}
7	91.7	101.7	TEW 2	TEW_{wide}
8	124.3	134.3	TEW 2	TEW_{wide}
9	97.7	101.7	TEW 2	TEW_{small}
10	124.3	128.3	TEW 2	TEW_{small}
11	146.0	187.6	Scatter 1	DEW_*k* factor
12	79.1	101.7	Scatter 2	DEW_*k* factor
13	208.4	250.0	Downscatter 1	DS
14	124.3	146.9	Downscatter 2	DS
15	187.6	208.4	Dual peak 1	DPW

DEW, dual-energy window; DPW, double-photopeak window; DS, downscatter; TEW, triple-energy window.

performed with more than the default three iterations and eight subsets – namely, with three iterations and 16 subsets and with four iterations and 16 subsets. One of the reconstructions was performed with eight iterations and 16 subsets.

Neither prefiltering nor postfiltering was applied. Attenuation correction was applied using a low-dose 140 kVp CT scan [15], which was transformed into an attenuation coefficient map for 100 keV photons, which subsequently was scaled to an attenuation map for

the 113 and 208 keV photons. As scatter correction techniques are applied, narrow beam attenuation coefficients are applied.

Scatter correction methods

In this section the different scatter correction methods are described using the following symbols:

(1) C for absolute number of counts;
(2) w for the window width in keV;
(3) c for the count concentration in counts/ml;
(4) V for the volume in ml;
(5) k for the multiplication factor.

The subscripts prim and total are used to refer to the primary (unscattered) photons and the total number of counts, respectively.

The following scatter correction methods were used in this study.

No scatter correction

For comparison we started with a basic SPECT reconstruction in which only attenuation correction was applied, based on the acquired CT scan [15]. No scatter correction was applied.

Effective scatter source estimation

The standard Philips scatter correction, which is based on the ESSE method, was also applied [16]. This method uses the concept of defining an effective source distribution of scatter, calculating the expected scatter projection data from this effective source of scatter photons and adding this calculated scatter projection data to the projection of the estimated image to produce the total estimated projection. The estimate of the scatter is calculated from the image estimate and density map by convolving the image estimate with a three-dimensional scatter convolution kernel. This convolution kernel is precalculated and depends on the photon energy [16]. No extra energy window, besides the main energy window, is needed for this correction method.

Triple-energy window

With the triple-energy window (TEW) method two small energy windows are defined around the main energy peak window. The two abutting windows are used to estimate the amount of scatter in the main window. Scatter correction was applied following [8,17]:

$$C_{\text{prim}} = C_{\text{total}} - \frac{1}{2}(k_{\text{lower}} \times C_{\text{lower}} + k_{\text{higher}} \times C_{\text{higher}}), \qquad k_{\text{i}} = \frac{w_{\text{prim}}}{w_{\text{i}}}, \tag{1}$$

where the subscript lower refers to the lower energy window and the subscript higher refers to the higher energy window. The subscript i is used to indicate an arbitrary window.

In the literature, different energy window widths are used [8,18–20]. Therefore, in this study two different versions of the TEW method were investigated. For this purpose two different sets of energy windows were defined, one with a width of 10 keV (windows 3 and 4, and windows 7 and 8) and one with a width of 4 keV (windows 5 and 6, and windows 9 and 10).

Dual-energy window

In the dual-energy window (DEW) method a broad window is defined below the main energy window with the same width. The assumption is that the spatial distribution of the scattered photons in the lower energy window is a good estimate of the distribution of the scattered photons in the main energy window. Subtraction is then applied in the following way [6]:

$$C_{\text{prim}} = C_{\text{total}} - k_{\text{s}} \times C_{\text{s}}, \tag{2}$$

where the subscript s is used to indicate the scatter window.

In the literature there is some discussion on the value of k that should be used. In the original paper of Jaszczak *et al.* [6] a factor of 0.5 was used for ^{99m}Tc, but in later papers, for example, in those by Koral *et al.* [21] and Luo *et al.* [22], it was stated that the multiplication factor is dependent on, among other things, the ratio of background activity (sphere vs. cylinder) and the volume of interest (VOI) size. Monte Carlo simulations suggested a multiplication factor of 0.43 [23]. The multiplication factors found in these studies were all for ^{99m}Tc. In this study we used three different multiplication factors to determine their influence on the corrected image: 0.5, 0.8 and 0.9. The value of 0.5 was used because it is the value most used in the literature, and the values of 0.8 and 0.9 were used on the basis of the ratio of the background activity and the VOI sizes as suggested by other studies such as the ones by Koral and colleagues [21,22,24].

Downscatter correction

To correct for downscatter a window above the main energy window was defined with the same width as the main energy window (windows 13 and 14). The corrected image was calculated as follows [25]:

$$C_{\text{prim}} = C_{\text{total}} - k_{\text{ds}} \times C_{\text{ds}}, \tag{3}$$

where the subscript ds is used to indicate the downscatter window.

To determine k_{ds} a VOI outside the phantom was drawn. In the projection data outside the phantom no primary photons are present. In contrast, downscattered photons can be detected if they penetrate through the septa of the collimator, while it is assumed that they are collimated perpendicular to the crystal surface. Alternatively, they can be backscattered into the crystal and detected outside the projection of the phantom.

Assuming that k_{ds} is space invariant (not depending on position), k_{ds} was calculated using the formula:

$$k_{ds} = \frac{\sum C_{total}}{\sum C_{ds}}. \quad (4)$$

In the case of imaging the 113 keV photons of ^{177}Lu, the 208 keV photons can downscatter into the 113 keV window. The 208 keV photons can scatter both inside the phantom and in the material behind the scintillation crystal. Backscattering (180°) of a 208 keV photon results in a photon of 115 keV, which is well inside the imaging window for the 113 keV photons.

Downscatter correction for the few percent 250 and 321 keV photons is not necessary in the case of imaging the 208 keV photons with medium-energy collimators

Combined scatter and downscatter correction

With the TEW method, correction for scatter and downscatter is applied, but with the DEW method only a part of the downscatter is taken into account. To compensate for downscatter as well, a combination of the DEW method and the downscatter correction method was applied. The used windows were 146–187.6 keV (window 11) with a *k*-factor (k_2) of 0.5 for the scatter correction and 208.4–250 keV (window 2) for the downscatter correction with the same *k*-factor (k_1) as used for downscatter alone for the 208.4 keV photon energy peak and 79.1–101.7 (window 12) and 124.3–146.9 (window 14) for the 113 keV photon energy peak. Because the scatter window is contaminated with downscatter as well, a correction factor k_3 is applied to correct for this. This correction factor k_3 is calculated in the same way as the *k*-factor for downscatter [see Eq. (4)], except for the fact that instead of the main energy window C_{prim} the scatter window C_s was used [26]. The final formula for obtaining the corrected image then becomes:

$$C_{prim} = C_{total} - (k_1 - k_2 \times k_3) C_{ds} - k_2 \times C_s. \quad (5)$$

Dual-photopeak window

Instead of measuring extra windows next to the main energy window to estimate the scatter in the main window, the information in the main window itself can be used. The dual-photopeak window (DPW) method is based on the fact that the lower part of the main energy window contains more scattered photons than the upper part (ratio α). In the study by Ljungberg *et al.* [27] the main energy window is split into two abutting nonoverlapping energy windows that are symmetrically located around the photopeak. The observed relative difference between the two windows is then used to calculate the scatter fraction, or the scatter-to-total ratio (STR). In this study we have used a method that is comparable to the one used in the study by Pretorius *et al.* [28] and is called the channel ratio method. Assuming that the contribution of the nonscattered photons to the upper and lower window is the same ($C_{prim}/2$), it can be derived from

$$C_{prim} = C_{total} - C_{total} \times STR, \quad (6)$$

with

$$STR = \frac{\alpha+1}{\alpha-1} \times \frac{C_{lower} - C_{higher}}{C_{lower} + C_{higher}}. \quad (7)$$

The value of α (the ratio between the scatter in the lower and the upper window) equals 3 in the case of a linear descending distribution of the scatter in the primary window.

The method by Pretorius *et al.* [28] is based on experimental determinations of the window weights, whereas Ljungberg *et al.* [27] have calculated a fit (based on Monte Carlo simulations) from which α can be determined. We determined α based on comparison with the formula used by Ljungberg *et al.* [27] and it was calculated to be 3.6, which is close to the value of a linear descending distribution.

Because the dual-peak method is highly noise sensitive [9], a spatial 3×3 filter with a Gaussian kernel (coefficients 1/4, 1/8 and 1/16) is applied before calculating the scatter fraction.

Because only 15 energy windows could be defined in the Philips scanner and because we do not expect the DPW to work properly in the 113 keV window because of the downscatter of the 208 keV photons that violates the assumption of the scatter distribution, we have chosen to define the DPW window only for the 208 keV window.

Analysis

VOIs were drawn around the six spheres and in the background of the phantom (Fig. 3).

In order to compensate for the partial volume effect and subjectivity, large volumes were drawn as proposed by Tossici-Bolt *et al.* [29]. The counts in the spheres (C_{sphere}) were calculated with:

$$C_{sphere} = C_{VOI} - C_{BG}(V_{VOI} - V_{sphere}), \quad (8)$$

where the subscript BG refers to the background. Note that the volume of the sphere is the outer volume including the cold walls. For all the different correction methods, the intensity ratios between the six spheres and the background were calculated and compared with the real value. The number of counts in the background outside the phantom was also obtained. If the correction methods work correctly, there should not be any counts there.

To be able to calculate the absorbed dose in a patient a conversion factor between the number of counts in the organ of interest and the activity is needed. This conversion factor is calculated in a phantom in which the activity and the uptake (100%) are known. To

Fig. 3

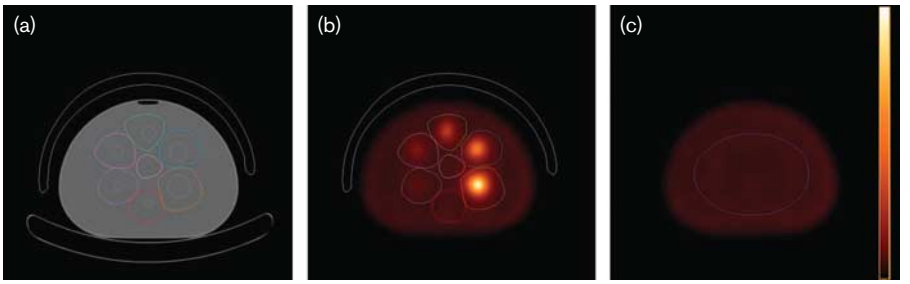

Two transaxial slices (medium-energy general purpose collimators and 208 keV energy window), reconstructed and both attenuation and scatter corrected with Astonish. (a) Low-dose computer tomography slice through the centre of the (visible) walls of the spheres and the volume of interest (VOIs) in different colours. (b) Single photon emission computer tomography (SPECT) of the same slice as in (a) with the VOIs shown in different colours. (c) SPECT slice in the phantom far away from the spheres illustrating the VOI for the background. The banana-like VOI outside the phantom is used for determination of the weight for certain energy window correction methods. Colour scales are linear with highest intensity at the top.

calculate the conversion factor the same VOIs are used as for calculating the ratios. The real activity was calculated on the basis of the measurements in a gamma counter, which in turn is calibrated against the dose calibrator used for the measurement of injected activity in phantoms and patients. Activity values are corrected for the decay time and the efficiency of the gamma counter itself. The conversion factor is obtained by dividing the real activity by the measured concentration in the sphere, corrected for the background activity.

Statistics

In order to compare the different methods with the reference value (the measured intensity ratio) analysis of variance tests were performed. If any significant ($P < 0.05$) difference was found between the groups a post-hoc Dunnett test (two-sided) was performed to compare with the reference value. Bonferroni tests were performed to compare the different variations of the methods with each other (e.g. TEW with small and broad windows). When the data were not normally distributed (tested with Kolomogorov–Smirnov) the Kruskal–Wallis test was applied instead of the analysis of variance. When the variances in the data differed significantly from each other, the Dunnett T3 test was performed instead of the Dunnett test.

Results

Comparison between the different scatter correction methods was performed for each collimator separately. Because the inaccuracy of the intensity ratio becomes larger when the sphere becomes smaller (because of partial volume effects and the limited amount of counts), the smallest two spheres are not taken into account for the comparisons. Figure 4 shows three SPECT reconstructions for both the 113 keV window with LEGP collimators and the 208 keV window with MEGP collimators to illustrate the influence of scatter and downscatter correction. Note that downscatter correction is not relevant for the 208 keV window. Figure 5 shows three SPECT reconstructions for both the 113 keV and 208 keV energy windows in order to illustrate the differences between the three collimators.

The results for the ratios are shown in Figs 6–9. Because of the high values for the ratios for $DEW_{0.9}$ these results are omitted from the figures, but are shown in Tables 3 and 4.

No significant differences were found between the two TEW methods (one with a small and one with a somewhat broader window) for any of the three collimators ($P = 1.000$).

For all the correction methods, the ratio between the counts outside the phantom and the background inside the phantom (a measure for the contribution of downscattered photons to the final images) was smaller than 10%, except for the TEW_{small} method in combination with the LEHR (12%) for the 113 keV window. For the MEGP collimator this ratio was below 1% for all correction methods.

There were no significant differences between the ratios for the images reconstructed with four and eight instead of three iterations and with 16 instead of eight subsets.

Significant differences were found between the DEW methods with different *k*-factors. Depending on the collimator used, this may result in overestimation and underestimation of the ratio.

Low-energy high resolution

The reconstruction of the higher energy window (around 208 keV) with the LEHR collimator gives artefacts, which results in ratios more than a factor 2 lower than the real value. Scatter correction methods were not applied to this window because of this problem.

Significant differences between the calculated ratio and the real ratio were found for the 208 keV window and for the 113 keV window without scatter correction. High relative SDs in the background volume were observed, with values above 15% even rising up to 49% for the DEW method with

Fig. 4

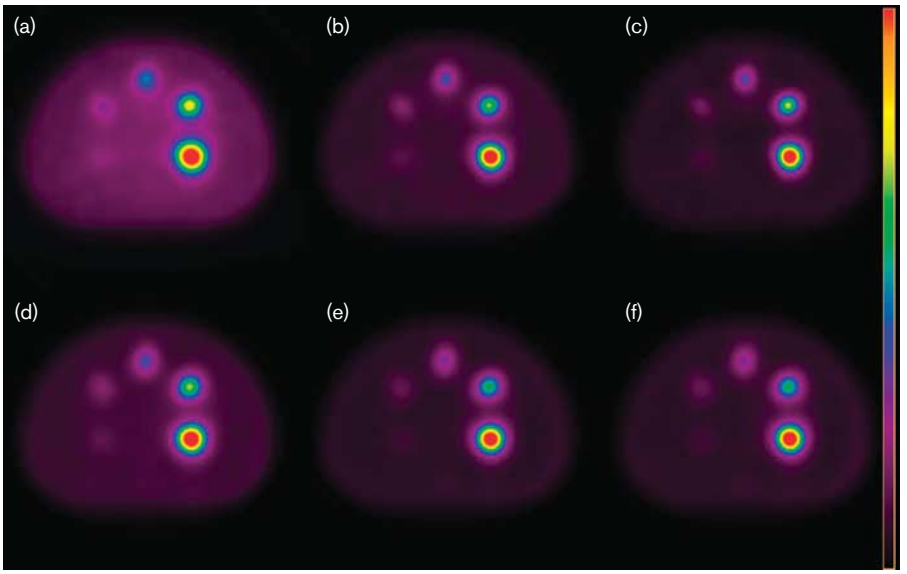

Six single photon emission computer tomography reconstructions [low-energy general purpose collimators for 113 keV (a, b, and c) and medium-energy general purpose for 208 keV (d, e, and f)] illustrating the effect of scatter and downscatter correction. (a, d) Slice through the centre of the spheres with attenuation correction only. (b, e) Same as (a) and (d) but with scatter correction with the dual-energy window method (weight factor of 0.5). (c, f) Same as (a) and (d) but with combined scatter and downscatter correction with the triple-energy window method with 'wide' energy windows. Colour scales are linear with highest intensity at the top.

Fig. 5

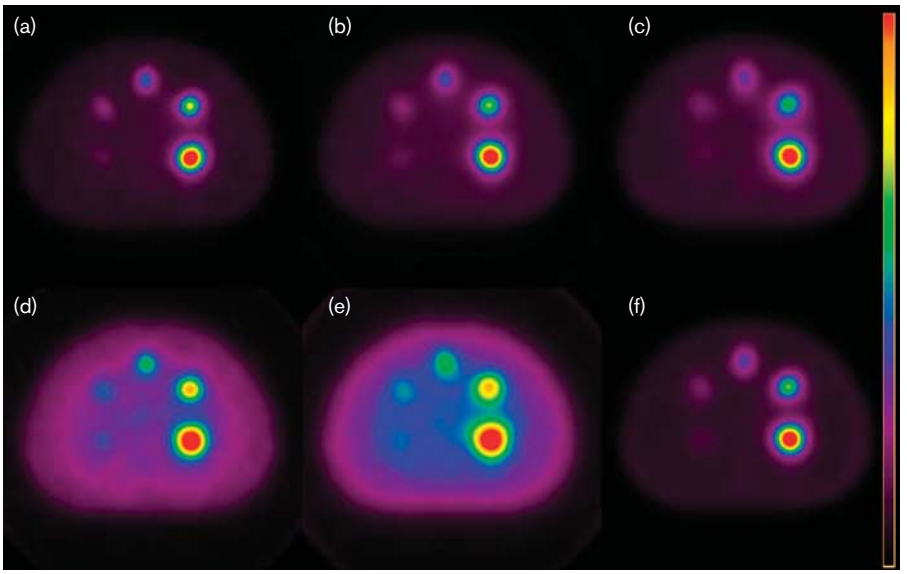

Reconstructions of the three collimators [low-energy high resolution (a, d), low-energy general purpose (b, e) and medium-energy general purpose (c, f)] for 113 keV (a, b, c) and 208 keV (d, e, f) energy windows. All slices are reconstructed with attenuation correction and the effective scatter source estimation method. Colour scales are linear with highest intensity at the top. Notice the low image quality for the 208 keV energy window with low-energy collimators due to septal penetration.

a k-factor of 0.9. For the LEHR collimator and the 113 keV imaging window the $DEW_{0.5}$ method and the combined downscatter and DEW method give similar values, because the downscatter correction in the DEW window is close to the amount of downscatter in the 113 keV imaging window. Figure 6 shows an overview of the results.

Fig. 6

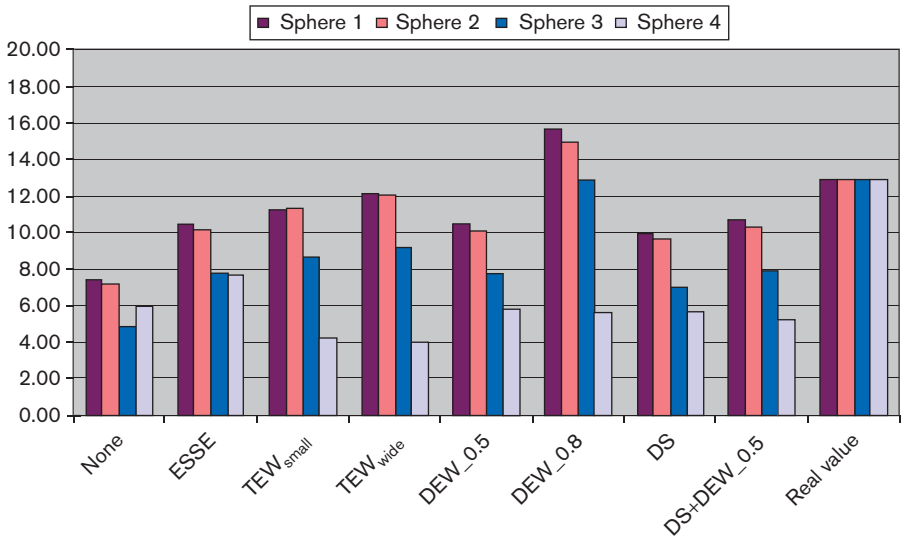

Results of the low-energy high resolution collimator for 113 keV. DEW, dual-energy window; DS, downscatter; ESSE, effective scatter source estimation; TEW, triple-energy window.

Fig. 7

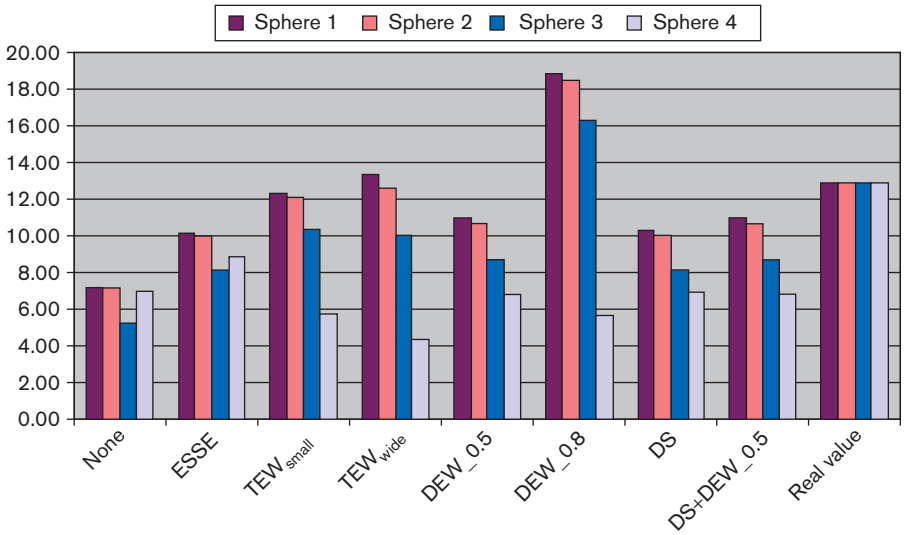

Results of the low-energy general purpose collimator for 113 keV. DEW, dual-energy window; DS, downscatter; ESSE, effective scatter source estimation; TEW, triple-energy window.

Low-energy general purpose

As for the LEHR collimator the reconstruction of the 208 keV window does not work well because of septal penetration of the primary imaging photons. Reconstruction with the scatter correction techniques was not applied because of this. For the LEGP collimator and the 113 keV imaging window the $DEW_{0.5}$ method and the combined downscatter and DEW method give exactly the same values, because the downscatter correction in the DEW window equals the amount of downscatter in the 113 keV imaging window.

The ratios obtained with 208 keV differ significantly from the real ratio. For the 113 keV window, only the method without scatter correction gives significantly different results from the real value. Figure 7 shows an overview of the results.

Fig. 8

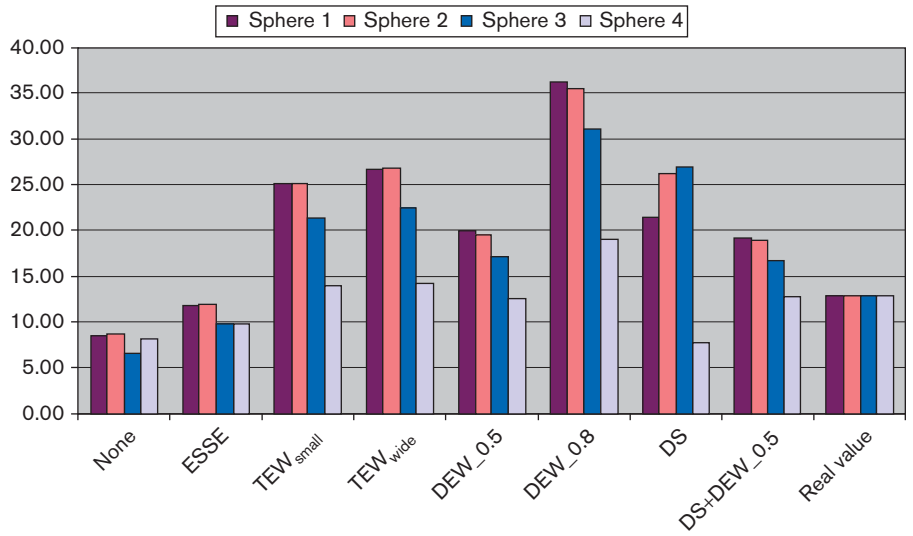

Results of the medium-energy general purpose collimator for 113 keV. DEW, dual-energy window; DS, downscatter; ESSE, effective scatter source estimation; TEW, triple-energy window.

Fig. 9

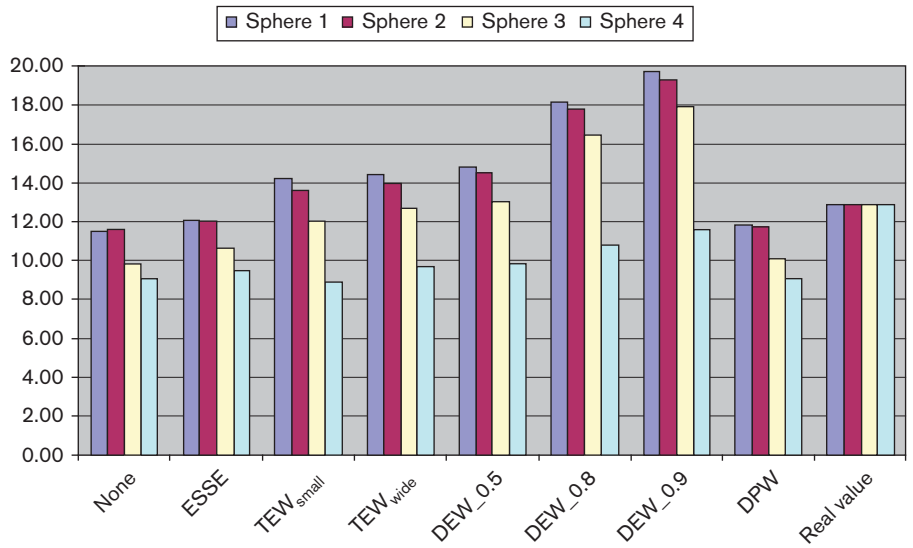

Results of the medium-energy general purpose collimator for 208 keV. DEW, dual-energy window; DS, downscatter; ESSE, effective scatter source estimation; TEW, triple-energy window.

Medium-energy general purpose

When the MEGP collimator is used the calculated ratios for the higher energy window are already close to the real ratio without applying scatter correction. When the standard scatter correction (ESSE) is used the calculated ratio for both the lower and the higher energy window is close to the real ratio. The other scatter correction methods tend to overestimate the ratio, especially in the lower energy window. The downscatter method does not work in the higher energy window, as there is no downscatter present in this situation, and it does not work in the case of the downscatter correction for 113 keV as in the study by de Nijs *et al.* [25], as the high-energy photons are collimated, and the weight cannot be determined outside the patient. Relative SDs of the background are high, especially for the

Table 3 Difference (%) between the real intensity ratio and the ratio of the largest sphere estimated after the different scatter correction methods for the three collimators

	LEHR	LEHR	MEGP	MEGP	MEGP	LEGP	LEGP
Energy window (keV)	113	208	113	208	113+208	113	208
None	−42.5±9.1	−66.0±13.2	−35.0±7.2	−10.9±9.7	−27.1±7.1	−44.1±7.5	−72.1±13.7
ESSE	−18.6±11.7	−64.7±12.5	−8.9±9.0	−6.6±9.4	−7.8±9.1	−21.3±7.4	−71.2±13.2
TEW_{small}	−12.9±25.8		94.2±40.9	10.5±18.5		−4.3±23.7	
TEW_{wide}	−5.4±29.7		107.0±46.1	12.0±16.6		3.7±31.7	
DEW, k=0.5	−18.4±17.0		53.8±26.3	15.0±17.7		−14.9±15.2	
DEW, k=0.8	21.7±35.9		180.5±61.8	40.9±26.6		46.9±48.5	
DEW, k=0.9	47.3±47.4		285.4±97.1	52.7±29.2		94.2±75.8	
DS1	−23.0±16.1		66.3±69.0	−102.0±73.6		−19.9±12.6	
DS1 + $DEW_{0.5}$	−16.6±19.7		47.9±22.7	16.3±16.7		−14.9±15.2	
DPW				−8.0±10.5			

The statistical uncertainty due to the noise of all calculated ratios is less than 2 percentage points. A minus sign indicates an underestimation. Standard deviation of the differences for the four largest spheres is given as ±SD.
DEW, dual-energy window; DPW, dual-photopeak window; DS, downscatter; ESSE, effective scatter source estimation; LEHR, low-energy high resolution; LEGP, low-energy general purpose; MEGP, medium-energy general purpose; TEW, triple-energy window.

Table 4 Conversion factor, in kBq/cps, of the largest sphere estimated after the different scatter correction methods for the three collimators

	LEHR	LEHR	MEGP	MEGP	MEGP	LEGP	LEGP
Energy window (keV)	113	208	113	208	113+208	113	208
None	7.2±1.7	6.8±12.6	5.1±0.7	7.6±0.9	3.1±0.4	4.5±0.8	4.5±8.4
ESSE	11.3±2.2	8.1±9.7	8.2±1.0	8.9±1.1	4.2±0.5	7.1±0.8	5.3±6.2
TEW_{small}	12.0±9.5		12.1±4.6	8.9±2.4		7.2±3.9	
TEW_{wide}	11.2±10.9		11.2±4.7	8.8±2.0		6.7±6.6	
DEW, k=0.5	9.3±3.5		9.2±2.5	8.5±2.0		5.8±1.7	
DEW, k=0.8	12.0±10.4		11.7±5.0	9.4±3.1		7.4±8.5	
DEW, k=0.9	13.5±15.0		13.1±7.5	9.8±3.2		8.6±18.3	
DS1[a]	9.3±3.3					5.7±1.3	
DS1 + $DEW_{0.5}$	9.7±4.7		8.9±2.1	7.8±1.7		5.8±1.7	
DPW				7.4±1.1			

The statistical uncertainty due to the noise of all calculated conversion factors is less than 2 percentage points. Standard deviation of the conversion factor for the four largest spheres is given as ± SD.
DEW, dual-energy window; DPW, dual-photopeak window; DS, downscatter; ESSE, effective scatter source estimation; LEHR, low-energy high resolution; LEGP, low-energy general purpose; MEGP, medium-energy general purpose; TEW, triple-energy window.
[a]The downscatter correction method does not work for collimated high-energy photons (MEGP).

113 keV window. Figures 8 and 9 show an overview of the results.

Table 3 shows an overview of the difference between the real intensity ratio and the estimated intensity ratio after the different scatter correction methods are applied for the three collimators used in this study.

Table 4 shows an overview of the conversion factors needed to calculate the observed activity concentration in a patient from the number of counts in the organ of interest after the different scatter correction methods are applied for the three collimators used in this study.

Equation (8) is used to calculate the statistical uncertainty due to the noise, expressed as the empirical SD of the calculated intensity ratio, based on VOI statistics. For the VOI statistics the data from the final reconstructed images are used, which include uncertainties due to, for example, counting statistics and reconstruction. For spheres 1–4 (which are the four largest spheres) this statistical uncertainty due to noise typically spanned from less than 0.1–0.4, respectively, except for the ratios determined with the TEW method for the MEGP collimator with 113 keV windows, in which these values were 0.2 and 0.7, respectively. The uncertainty for the DEW method with 113 keV windows was up to 1.8 for sphere 4 because of failure of this method. However, the relative uncertainty was still less than 8%. The statistical uncertainty due to noise in spheres 5 and 6 can be more than 20% depending on the correction method. Image deterioration caused by noise was not investigated.

Discussion

In this study different scatter correction methods based on energy window subtraction are compared with each other in an experimental ^{177}Lu SPECT study for three different collimators. For ^{177}Lu imaging the MEGP collimator is advised. Both energy peaks could be used when the standard scatter correction technique (ESSE) was applied. The difference between the calculated ratio and the real ratio was less than 10% for both the low-energy and the high-energy window and when both windows were combined. Using one appropriate conversion factor (common for all spheres) both the 208 and the 113 keV imaging window can be utilized on their own or combined after reconstruction.

As expected, the reconstruction of the higher energy window (208 keV) is incorrect for the two low-energy collimators because of septal penetration. This leads to 'leaking' of information into neighbouring pixels, which renders accurate calculation of ratios and doses impossible. Applying scatter correction techniques is useless in this case.

Large differences were observed in the ratios calculated for the different spheres, especially for the low-energy window (113 keV). The high relative SDs in the background influence the accuracy of the obtained concentrations. Small differences in the background concentration can highly influence the obtained concentration ratio, especially in the smaller spheres, which might explain the differences between the spheres. Differences in the ratio of the spheres also mean different conversion factors for different sizes of spheres. In patients, the size of the tumour is normally not known, which implies that only one conversion factor, suitable for all tumour/organ sizes, can be used. Therefore, only methods that yield the same value for each sphere can be used for accurate dosimetry.

For some of the methods, several variations were also tested. For the TEW method, two different energy windows widths were tested, one smaller with a width of 4 keV and one somewhat broader, with a width of 10 keV. Both methods performed comparably. Because the TEW method is noise sensitive [7], which is especially a problem in dynamic SPECT studies [30,31] in which few counts are acquired, the TEW method with the broader windows might be more stable for dynamic studies.

For the DEW method different *k*-factors were tested. Statistically significantly different results were obtained with these methods. Which method performs best depends on which collimator is used. From the literature [21,22] it has become clear that the *k*-factor used depends on different factors. Koral *et al.* [21] found that the *k*-factor decreased as the background concentration increased. The size of the VOI also influences the *k*-factor, but its influence is dependent on the background concentration. When the background concentration is low, the *k* value drops rapidly with increasing VOI size, but *k* is almost constant when the background concentration is large. With the VOI size and background-to-sphere activity that were used in this study, a *k*-factor of around 0.5 should be appropriate. Unfortunately, Koral *et al.* [21] investigated the *k*-factor only for ^{99m}Tc and an LEGP collimator. Luo *et al.* [22] investigated the *k*-factor for ^{99m}Tc and ^{123}I, but a different phantom was used, which influences the value of the *k*-factor. Our study of ^{177}Lu suggests that for the 113 keV photons a *k*-factor of 0.5 for all collimators might be feasible. This *k*-factor of 0.5 also holds for the 208 keV photons with the MEGP collimator. The disadvantage of optimizing this *k*-factor is that this is only possible with experimental or simulation studies and that the values obtained might differ from the values that are needed in patients because the ratio between the VOI and the background in patients is not known beforehand.

Standard (down)scatter correction methods such as TEW and DEW do not work very well for lutetium for various reasons. The problem with the DEW method in the 113 keV window might be that characteristic radiation from the collimator lead (energies between 72 and 88 keV) deteriorates the DEW. In the case of imaging of the 208 keV photons the TEW method might be changed to a DEW method with one small window, because the upper window will mostly contain noise, which influences the accuracy of the method. Downscatter correction in the 208 keV window is not really necessary because almost no downscatter will be present in this window as a result of the very low abundance (few per cent compared with the 208 keV photons) of the higher energy photons. When correction with this method is applied, the calculated ratio differs considerably from the real ratio. This might be due to large uncertainties arising from the noise in determining the *k*-factor when no downscatter is present. When the MEGP collimator is used, large differences occur between the different scatter correction methods, but most of them are not significantly different from the real value. This might be due to the large variances obtained.

The DPW for the 208 keV window and the standard scatter correction technique (ESSE) for both the 113 and the 208 keV window perform best with MEGP collimators. When ESSE is used, the difference between the real ratio and the calculated ratio is small, and the differences between the spheres are small. When the DPW method is used, the differences between the different sized spheres are larger, which is reflected by a larger SD.

Only 15 energy windows could be defined in the Philips scanner. Because we did not expect the DPW to work properly in the 113 keV window as a result of the downscatter of the 208 keV photons that violates the assumption of the scatter distribution, we chose to define the DPW window for the 208 keV window only. The DPW method is sensitive to deviations of the energy calibration of the scanner [32], as it is based on dividing the main energy window into two parts with the limit placed exactly at the imaged photon energy, and it is noise sensitive [9]. In practice, this can be an important source of error. Furthermore, the DPW method is possibly unstable [33].

A ratio for the smaller spheres (mainly spheres 5 and 6) cannot be obtained, which means that dosimetry in small tumours/organs will fail as well. There are two main reasons for this: the influence of the partial volume effect will be larger in smaller objects because of the resolution limit of the scanner, and the number of counts will be lower, which makes the measurement less precise. The phantom corresponds to a patient of about 70 kg.

As the resolution of the reconstructed images depends on the collimator source distance, the resolution will be worse for larger patients and consequently the minimal detectable tumour size will be larger.

For ^{177}Lu imaging the MEGP collimator is advised. Both 113 and 208 keV energy windows can be used when the standard scatter correction technique (ESSE) is applied. The difference between the calculated ratio and the real ratio is less than 10% for both energy windows and when both windows are combined after reconstruction. When this method is used one conversion factor can be used for all the spheres, which makes accurate dosimetry feasible.

Acknowledgements

Conflicts of interest

There are no conflicts of interest.

References

1 Kwekkeboom DJ, Bakker WH, Kooij PP, Konijnenberg MW, Srinivasan A, Erion JL, *et al.* [^{177}Lu-DOTAOTyr3]octreotate: comparison with [^{111}In-DTPAo]octreotide in patients. *Eur J Nucl Med* 2001; **28**:1319–1325.

2 Pereira JM, Stabin MG, Lima FR, Guimaraes MI, Forrester JW. Image quantification for radiation dose calculations – limitations and uncertainties. *Health Phys* 2010; **99**:688–701.

3 Muller C, Forrer F, Bernard BF, Melis M, Konijnenberg M, Krenning EP, *et al.* Diagnostic versus therapeutic doses of [(177)Lu-DOTA-Tyr(3)]-octreotate: uptake and dosimetry in somatostatin receptor-positive tumors and normal organs. *Cancer Biother Radiopharm* 2007; **22**:151–159.

4 Sandstrom M, Garske U, Granberg D, Sundin A, Lundqvist H. Individualized dosimetry in patients undergoing therapy with (177)Lu-DOTA-D-Phe (1)-Tyr (3)-octreotate. *Eur J Nucl Med Mol Imaging* 2010; **37**:212–225.

5 Sward C, Bernhardt P, Ahlman H, Wangberg B, Forssell-Aronsson E, Larsson M, *et al.* [^{177}Lu-DOTA 0-Tyr 3]-octreotate treatment in patients with disseminated gastroenteropancreatic neuroendocrine tumors: the value of measuring absorbed dose to the kidney. *World J Surg* 2010; **34**: 1368–1372.

6 Jaszczak RJ, Greer KL, Floyd CE Jr, Harris CC, Coleman RE. Improved SPECT quantification using compensation for scattered photons. *J Nucl Med* 1984; **25**:893–900.

7 Buvat I, Benali H, Todd-Pokropek A, Di PR. Scatter correction in scintigraphy: the state of the art. *Eur J Nucl Med* 1994; **21**:675–694.

8 Ichihara T, Ogawa K, Motomura N, Kubo A, Hashimoto S. Compton scatter compensation using the triple-energy window method for single- and dual-isotope SPECT. *J Nucl Med* 1993; **34**:2216–2221.

9 King MA, Hademenos GJ, Glick SJ. A dual-photopeak window method for scatter correction. *J Nucl Med* 1992; **33**:605–612.

10 Small AD, Prosser J, Motherwell DW, McCurrach GM, Fletcher AM, Martin W. Downscatter correction and choice of collimator in ^{123}I imaging. *Phys Med Biol* 2006; **51**:N307–N311.

11 Lagerburg V, de Nijs R, Holm S, Svarer C. A comparison of different energy window subtraction methods to correct for scatter and downscatter in I-123 SPECT imaging. *Nucl Med Commun* 2012; **33**:708–718.

12 Larsson A, Ljungberg M, Mo SJ, Riklund K, Johansson L. Correction for scatter and septal penetration using convolution subtraction methods and model-based compensation in ^{123}I brain SPECT imaging – a Monte Carlo study. *Phys Med Biol* 2006; **51**:5753–5767.

13 Beauregard JM, Hofman MS, Pereira JM, Eu P, Hicks RJ. Quantitative (177)Lu SPECT (QSPECT) imaging using a commercially available SPECT/CT system. *Cancer Imaging* 2011; **11**:56–66.

14 Hudson HM, Larkin RS. Accelerated image reconstruction using ordered subsets of projection data. *IEEE Trans Med Imaging* 1994; **13**:601–609.

15 Khalil MM. *Basic sciences of nuclear medicine*. Berlin, Germany: Springer; 2010; p. 423.

16 Kadrmas DJ, Frey EC, Karimi SS, Tsui BM. Fast implementations of reconstruction-based scatter compensation in fully 3D SPECT image reconstruction. *Phys Med Biol* 1998; **43**:857–873.

17 Ogawa K, Harata Y, Ichihara T, Kubo A, Hashimoto S. A practical method for position-dependent Compton-scatter correction in single photon emission CT. *IEEE Trans Med Imaging* 1991; **10**:408–412.

18 Hashimoto J, Sammiya T, Ogasawara K, Kubo A, Ogawa K, Ichihara T, *et al.* Scatter and attenuation correction for quantitative myocardial SPECT imaging. *Kaku Igaku* 1996; **33**:1015–1019.

19 Nakajima K, Matsubara K, Ishikawa T, Motomura N, Maeda R, Akhter N, *et al.* Correction of iodine-123-labeled meta-iodobenzylguanidine uptake with multi-window methods for standardization of the heart-to-mediastinum ratio. *J Nucl Cardiol* 2007; **14**:843–851.

20 Verberne HJ, Feenstra C, de Jong WM, Somsen GA, van Eck-Smit BL, Busemann SE. Influence of collimator choice and simulated clinical conditions on ^{123}I-MIBG heart/mediastinum ratios: a phantom study. *Eur J Nucl Med Mol Imaging* 2005; **32**:1100–1107.

21 Koral KF, Swailem FM, Buchbinder S, Clinthorne NH, Rogers WL, Tsui BM. SPECT dual-energy-window Compton correction: scatter multiplier required for quantification. *J Nucl Med* 1990; **31**:90–98.

22 Luo JQ, Koral KF, Ljungberg M, Floyd CE Jr, Jaszczak RJA. Monte Carlo investigation of dual-energy-window scatter correction for volume-of-interest quantification in ^{99m}Tc SPECT. *Phys Med Biol* 1995; **40**:181–199.

23 Gustafsson A, Arlig A, Jacobsson L, Ljungberg M, Wikkelso C. Dual-window scatter correction and energy window setting in cerebral blood flow SPECT: a Monte Carlo study. *Phys Med Biol* 2000; **45**:3431–3440.

24 Luo JQ, Koral KF. Background-adaptive dual-energy-window correction for Compton-scattering in SPECT. *Nucl Instr Meth Phys Res* 1994; **353**:340–343.

25 de Nijs R, Holm S, Thomsen G, Ziebell M, Svarer C. Experimental determination of the weighting factor for the energy window subtraction-based downscatter correction for I-123 in brain SPECT studies. *J Med Phys* 2010; **35**:215–222.

26 de Nijs R, Svarer C. Combined backscatter and scatter correction for low count I-123 SPECT studies. *J Nucl Med* 2007; **48 (S1)**:424.

27 Ljungberg M, King MA, Hademenos GJ, Strand SE. Comparison of four scatter correction methods using Monte Carlo simulated source distributions. *J Nucl Med* 1994; **35**:143–151.

28 Pretorius PH, van Rensburg AJ, van AA, Lotter MG, Serfontein DE, Herbst CP. The channel ratio method of scatter correction for radionuclide image quantitation. *J Nucl Med* 1993; **34**:330–335.

29 Tossici-Bolt L, Hoffmann SM, Kemp PM, Mehta RL, Fleming JS. Quantification of [^{123}I]FP-CIT SPECT brain images: an accurate technique for measurement of the specific binding ratio. *Eur J Nucl Med Mol Imaging* 2006; **33**:1491–1499.

30 Pinborg L, Ziebell M, Frokjaer V, de Nijs R, Haugbol S, Yndgaard S, *et al.* Quantification of ^{123}I-PE2I binding to dopamine transporter with SPECT after bolus and bolus/infusion. *J Nucl Med* 2005; **46**:1119–1127.

31 Frokjaer VG, Pinborg LH, Madsen J, de Nijs R, Svarer C, Wagner A, *et al.* Evaluation of the serotonin transporter ligand ^{123}I-ADAM for SPECT studies on humans. *J Nucl Med* 2008; **49**:247–254.

32 Buvat I, Rodriguez-Villafuerte M, Todd-Pokropek A, Benali H, Di PR. Comparative assessment of nine scatter correction methods based on spectral analysis using Monte Carlo simulations. *J Nucl Med* 1995; **36**:1476–1488.

33 Zimmerman RE, Williams BB, Chan KH, Moore SC, Kijewski MF. Limitations of dual-photopeak window scatter correction for brain imaging. *J Nucl Med* 1997; **38**:1902–1906.